We are IntechOpen,
the world's leading publisher of
Open Access books
Built by scientists, for scientists

4,800
Open access books available

122,000
International authors and editors

135M
Downloads

154
Countries delivered to

Our authors are among the

TOP 1%
most cited scientists

12.2%
Contributors from top 500 universities

BOOK CITATION INDEX
CLARIVATE ANALYTICS
INDEXED

WEB OF SCIENCE™

Selection of our books indexed in the Book Citation Index
in Web of Science™ Core Collection (BKCI)

Interested in publishing with us?
Contact book.department@intechopen.com

Numbers displayed above are based on latest data collected.
For more information visit www.intechopen.com

A Sensors System for Indoor Localisation of a Moving Target Based on Infrared Pattern Recognition

Nikos Petrellis, Nikos Konofaos and George Alexiou
Computer Engineering and Informatics Dept., University of Patras
Greece

1. Introduction

Estimating the position of a robot, a vehicle or a person in an indoor area is a significant issue for a number of applications in Robotics, Automation and Ubiquitous/Pervasive Computing. Several approaches have already been proposed in order to locate indoors the position of a moving target. These approaches rely on a wide range of media including RF signals, lasers, ultrasound, magnetic fields, visible light, infrared beams, speedometers etc. A combination of heterogeneous approaches is often adopted (Borenstein et al., 1996) in order to increase the accuracy of the position estimation.

Cameras are widely used in a number of robotics applications (Jin et al, 2004); (Porta & Krose, 2006); (Clerentin et al, 2005); (Kzecka et al, 2005); (Gramegna et al, 2004); (Arras et al, 2001). The views captured by these cameras are processed in order to locate scale invariant landmarks that indicate the position of the robot in a familiar area (Tovar et al, 2006). Moreover, the function of the human eyes can be imitated by a pair of cameras focusing at the same direction (Se et al, 2002). The shape, the depth and the distance of the surrounding objects may be estimated by comparing the images retrieved by these cameras. It is obvious that both the computational and the architectural cost of such a solution is high.

Laser scanning is often used in conjunction with the image processing techniques mentioned above (Miura et al, 2006); (Clerentin et al, 2005); (Victorino et al, 2003); (Arras et al, 2001); (Thrun, 2001). A rotating beacon is transmitting a laser beam which is reflected by the surrounding objects. The round trip time of the signal can be used for the estimation of the distance between the target and an object (e.g., a wall). An ultra high speed controller connected to sensors with fast response is required in this case, since the laser travels with the speed of light and the slightest deviation in the measured time intervals would fail to estimate the distance with adequate accuracy. The strength of the reflected beam may also provide an indication of the distance between the target and an object.

In a similar way, sonar or ultrasonic waves can be used instead of lasers (Jin et al, 2004); (Bicho, 2000); (Minami et al, 2004); (Holmberg, 1994); (Ullate, 1993) . In this case, it is easier to measure the round trip time of the reflected wave since it travels with a significantly lower speed than the laser but the sound can not be treated as a directional beam. Moreover, it is difficult to isolate the sonar transmitter from the receiver. In other words, the receiver cannot be sure if it "listens" to a reflected sound wave or to a sound coming from the sound

source itself. The distance that can be measured using sonar data is of the order of several centimetres.

Another popular indoor and outdoor localisation method relies on the signal strength of multiple transmitters (Ladd et al, 2005); (Flora et al, 2005). For example, the Received Signal Strength Indication (RSSI) of the Wireless Local Access Network (WLAN) or Bluetooth networks can be used to estimate the distance of a mobile computer from an Access Point. Another example of this approach concerns the position estimation of a user in a cellular phone network. The signal of the three RF base stations: *B1, B2* and *B3* of Fig. 1 is received at the target with different strength. The strength of each signal indicates the distance of the target from the corresponding base station (*d1, d2* and *d3* from *B1, B2* and *B3* respectively). The point where the three circles centred at *B1, B2* and *B3* (with radius *d1, d2* and *d3* respectively), intersect is the real position of the target. The estimation accuracy depends on the precision that the signal strength can be measured. Although the existing infrastructure of the base stations can be exploited, expensive high precision analogue sensors are required at the side of the target.
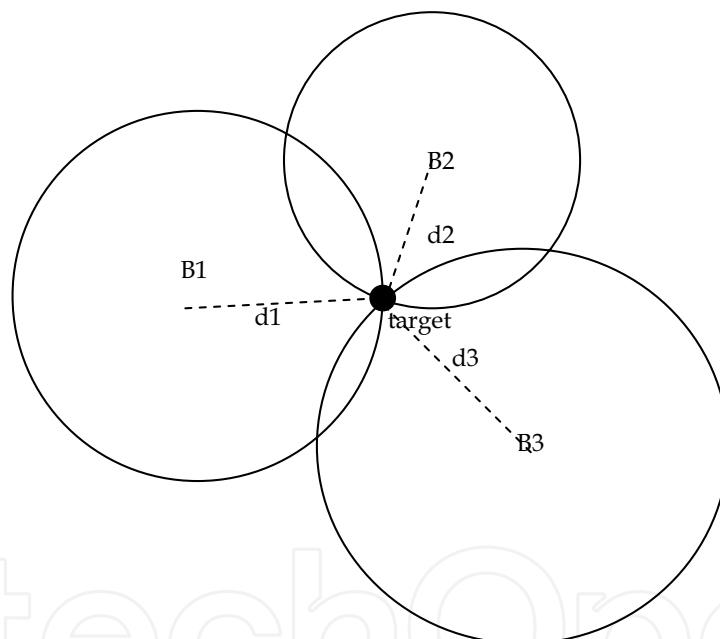

Fig. 1. Position estimation using the triangulation method

Magnetic fields have also been employed in order to accurately control in a non-contact way some machinery tools or medical instrumentation (Schlageter et al, 2001); (Kosel et al, 2005); (Arana et al, 2005). The distances covered in these cases range from a few millimetres to several tenths of centimetres. Nevertheless, distance estimation of up to 10m has also been reported in (Prigge & How, 2004).

Passive and active Infrared sensors have been employed in order to estimate distances of less than one meter (Jin et al, 2004); (Bicho, 2000). Infrared scanning is performed in the

same way as laser scanning. Additional properties of the object that is scanned can also be identified including surface shape and texture (Aytac & Barshan, 2004); (Benet et al, 2002); (Novotny & Ferrier, 1999).

An **absolute** position estimation method locates the current position of the target regardless of his previous movements. All the aforementioned methods can be considered as absolute. A **relative** position estimation approach is based on measuring how much distance has been walked since the last observation and in which direction. This kind of information can be retrieved by monitoring the speed and the steering of a vehicle (Jin et al, 2004); (Victorino et al, 2003); (Thrun, 2001). Stochastic processing can also be applied in order to evaluate how possible an estimated position is.

The position localisation method presented in this chapter is based on the statistical processing of digital infrared patterns that are received at the target (Petrellis et al, 2005); (Petrellis et al, 2006). These patterns are transmitted by at least two infrared emitting devices positioned at the borders of the covered area at a proper topology. The various supported pattern types are recognised with a different "success rate" at the target according to its current position. The term "success rate" refers to the number of patterns received compared to the expected ones for a specific type. The success rates of all the supported pattern types form a multidimensional identity of a specific position. The digital processing of the infrared patterns is carried out by an ultra low cost system since neither high precision sensors nor high speed controllers are required.

The target familiarises with the environment by visiting specific positions during a calibration stage. The reflections caused on the surrounding objects and walls are static and dynamic. The static reflections are encountered during the calibration stage and are exploited as an additional dimension to the position identity. The dynamic reflections caused by obstacles or persons that instantly appear in the covered area during real time operation can be considered as unpredictable dynamic noise. In order to overcome the effect of this noise a number of rules that confine the acceptable future positions can be applied.

The interference of other infrared sources like sunlight are avoided by sending the infrared patterns over a carrier. The frequency of the carrier determines how fast a position estimation can be carried out. If a standard 38KHz carrier is selected, the time needed for a position estimation exceeds 1sec. This time can be reduced to less than 100ms if a 1MHz carrier is used instead. The area covered by two infrared transmitters is more than 15m² and can be further expanded if additional transmitters are used in a proper topology. The absolute position estimation error is less than 10cm in most of the covered area (Petrellis et al 2006b).

2. System Architecture and Setup

The architecture of the infrared pattern transmitter (IRTX) used in our system is presented in Fig. 2. A control unit generates the digital pattern signal. This signal is mixed with the carrier and the amplified output drives the infrared emitting diode. The carrier can be generated either by the control unit or by an external square wave generator. The power dissipation and the beam angle of the emitting diode is a significant issue since it is desirable to cover a wide enough area. In order to achieve this goal, more than one diodes can be connected in parallel (Fig. 2), positioned in a circular arrangement. If more than one IRTX devices are used they may share the same control unit if wiring is not an issue.
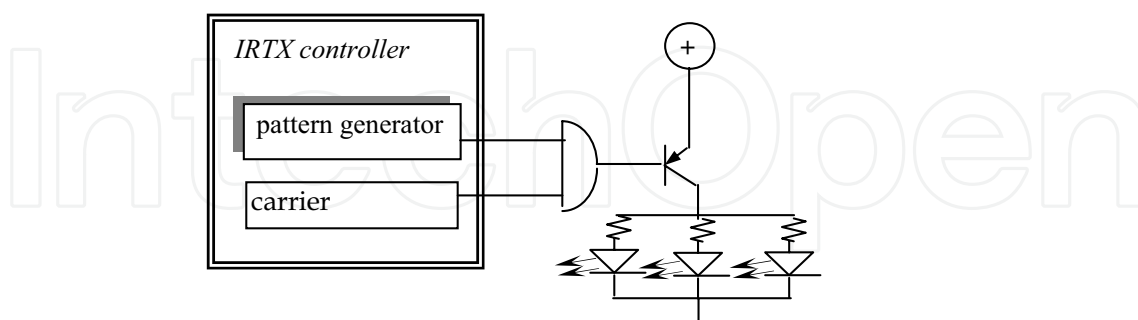
Fig. 2. The architecture of the IRTX device

The structure of an infrared pattern is presented in Fig. 3. Each pattern consists of a series of n identical pulses with period equal to $H+L$. The specific pattern type is named MODn. If $i \neq j$, the pattern types MODi and MODj should be recognised with different degree of difficulty at the receiver. The parameters H and L are chosen longer for MODi than MODj for $i<j$. In this way, the MODi patterns are received without errors in longer distance than MODj since it has longer and smaller number of pulses. The transmission starts with a preamble that can be a special code or a long enough pause interval. Then, a set of M identical patterns of each supported type is transmitted. The successive patterns are separated by a pause interval P longer than H or L. This procedure is repeated by sending a new preamble. The success rate of a pattern type is defined as the number of patterns received compared to the number of the expected ones (M).
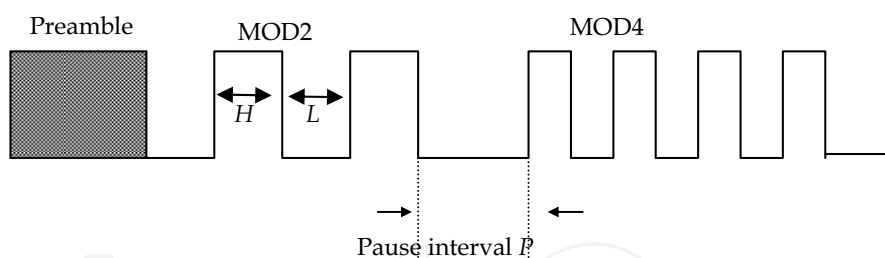

Fig. 3. The structure of the digital infrared patterns

The architecture of an infrared receiver (IRRX) is presented in Fig. 4. The modulated signal received by the infrared sensor is driven to a bandpass filter that allows only the pulses that are modulated at the specific carrier frequency. Then, an integrator rejects the carrier and the resulting digital pulses are sampled directly by a controller that recognises the pattern types from the pulses and the pause intervals. The number of patterns of a specific type that were recognised between two successive preambles is the success rate of this type and can be directly used to estimate the current position. The estimation can be carried out by the control unit itself or by a host computer that communicates with the controller and uses the

estimation results at the target application. At our experimental setup, the controller is connected to a laptop through a serial port. A custom application running at the laptop is performing the position estimation algorithm and presents the position estimation results.
Two IRRX devices are connected to the controller at the side of the target facing opposite directions. The orientation of these IRRX devices should be kept stable, because a slight rotation may drastically affect the success rates measured and the consequent position estimation results. At the present setup, it is assumed that the target can move on a plane but can not rotate i.e., it has two degrees of freedom. Nevertheless, the target may be allowed to rotate around itself if this can be done independently of the IRRX devices.
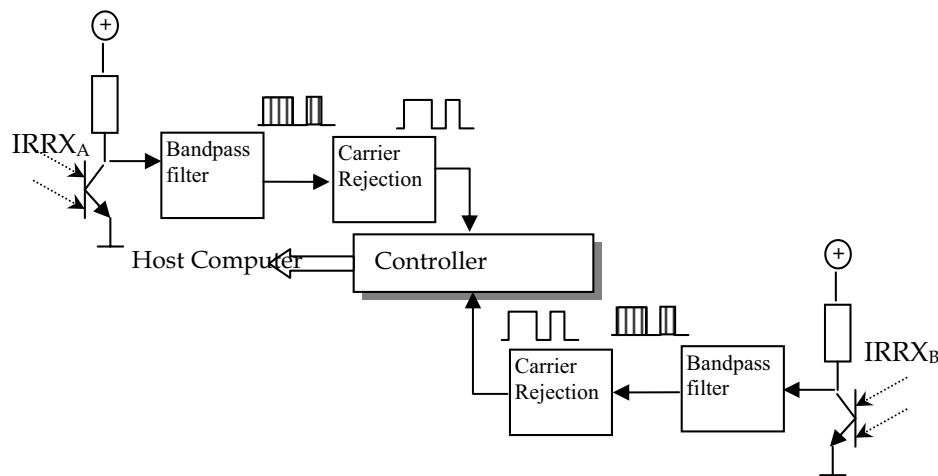

Fig. 4. The architecture of the IRRX devices.

3. Position Estimation Method

The success rate r_i of the MODi type, is the number of MODi patterns retrieved between two successive preambles. A calibration stage is necessary before the real time operation in order to familiarise with the environment. During this stage, the target visits specific positions in the covered area and records the retrieved success rate. If the topology of Fig. 5 is assumed, the target visits positions in regular distance and angular steps around an IRTX device. The success rates measured for a specific angular displacement can be drawn as a function of the distance as shown in Fig. 6.
The discrete values measured during the calibration can be approximated by a continuous non linear model like Richards' (Bates & Watts, 1988), before the real time operation of the system:

$$r_i = p_1 /(1 + e^{-p_2(d-p_3)})^{1/p_4}$$
(1)

The success rate r_i is approximated as a function of the distance d for a specific angle, while the parameters p_1, p_2, p_3 and p_4 are estimated by an external off the shelf optimisation tool. If the IRTX device supports k types of patterns, the calibration is performed in l directions and m positions are visited in each direction, then a set of $k \cdot l \cdot m$ equations like (1) have to be

estimated. In fact, only the parameters p_i have to be stored requiring a memory of $4 \cdot k \cdot l \cdot m$ floating point values.
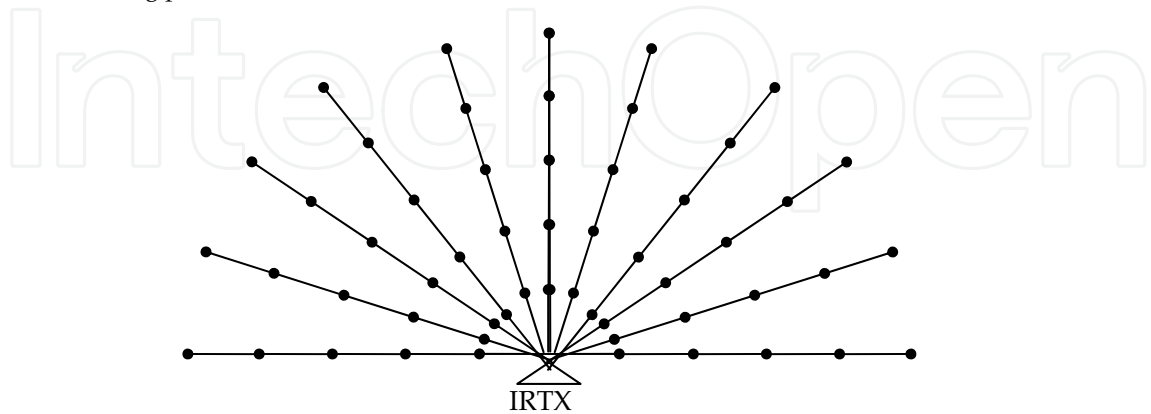

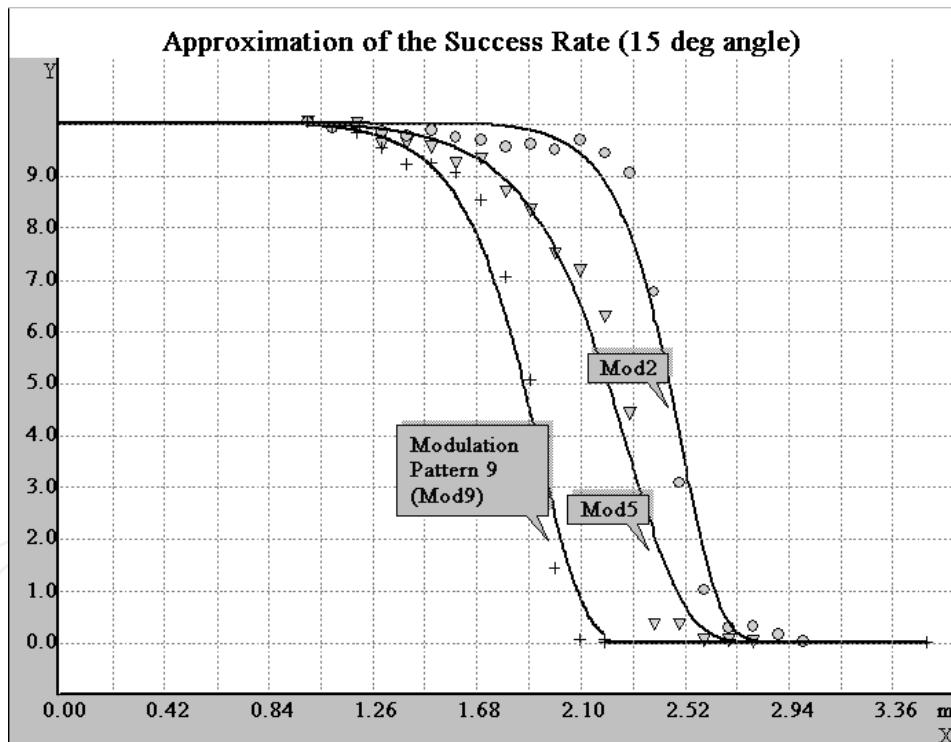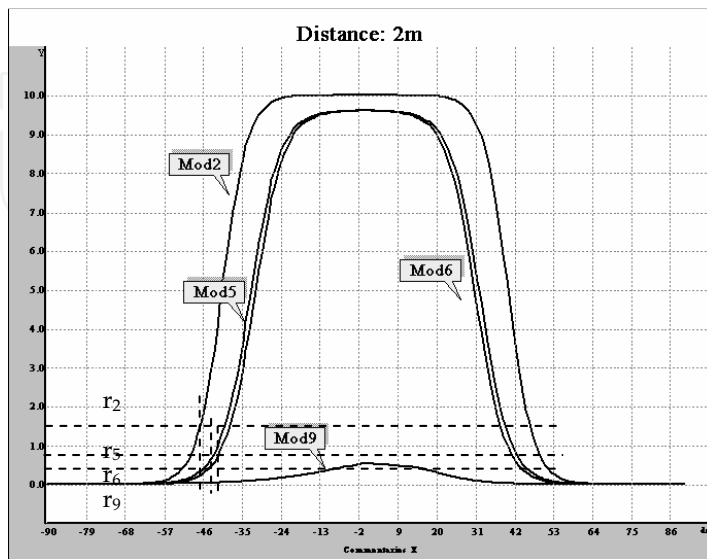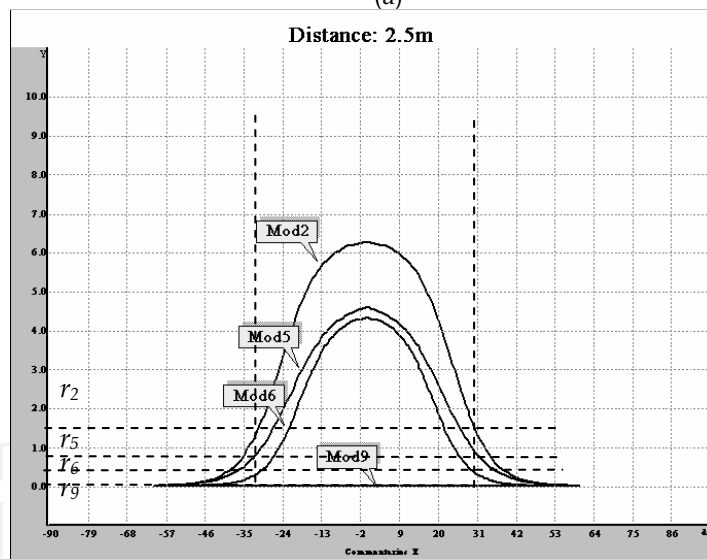Fig. 5. Calibration at regular angle and distance steps.

Fig. 6. Approximation of the calibration values with a nonlinear model (Petrellis et al 2006a).

Alternatively, the success rates for a specific distance can be drawn as a function of the angular displacement as shown in Fig. 7.

(a)

(b)

Fig. 7. The success rates as a function of the angular displacement for a specific distance
(Petrellis et al 2006a).

The polar coordinates of the target related to the IRTX device can be estimated as follows
(Petrellis et al, 2006a): if the pattern types MOD2, MOD5, MOD6 and MOD9 are supported
by the IRTX device of Fig. 5 and the success rates r_2, r_5, r_6 and r_9 are retrieved by the target
at a specific position during real time operation then the curve sets of all the specific
distances have to be checked out. For example, if the set of curves at a distance of 2m are

used, the success rate values do not converge to the same angular displacement (Fig. 7a). On the contrary, if the curves retrieved at a distance of 2.5m are used, the measured r_i values converge to a ±30° angular displacement (Fig. 7b). The ambiguity of whether the target is located at the right or at the left side of the IRTX device can be clarified if a second IRTX device is positioned in a topology like the one presented in Fig. 8. Hence, the IRTX2 device is used in order to break the symmetry and extend the covered area.
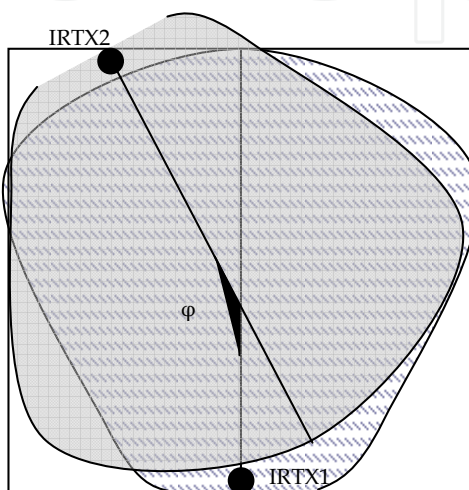

Fig. 8. Placing a second IRTX device in the covered area.

The approach described above suffers from two important drawbacks. First of all, the reflections from the surrounding area have to be negligible. Otherwise, the behaviour of the success rate is not similar to the one presented in Fig. 6 and 7 and a unique model like Richards' is not applicable. For the same reason, the two IRTX devices should not transmit their patterns concurrently in order to avoid scrambling.

These limitations can be overcome if the calibration and position estimation method is based on a grid (Petrellis et al, 2006b). The grid plane extends to all the covered area. During the calibration stage, the target visits the grid nodes and registers the retrieved success rates in the vectors *A, B, A′* and *B′*. The patterns retrieved "in order" by the IRRX$_A$ device are stored in *A* while patterns that are recognised "out of order" by the same device are stored in *A′*. In a similar way, the vectors *B* and *B′* refer to patterns that are received by the terminal IRRX$_B$. For example, if the IRRX$_A$ device points towards the IRTX1 that supports the pattern types MOD3, MOD4, MOD7 and MOD8, then the vector positions *A[3], A[4], A[7]* and *A[8]* store the corresponding number of patterns received "in order" between two preambles. If the IRTX2 device supports MOD2, MOD5, MOD6 and MOD9 types, the corresponding vector positions for the patterns received "in order" are *B[2], B[5], B[6]* and *B[9]* since IRRX$_B$ is facing towards IRTX2. Nevertheless, IRRX$_A$ may also receive patterns transmitted by IRTX2 through reflections. The corresponding number of patterns are stored in *A[2], A[5], A[6]* and *A[9]* and are viewed as "unexpected".

The success rate vectors *A, A', B* and *B'* form the identity of a position. The reflections and the scrambling are encountered as different dimensions in these vectors ("expected", "unexpected" and "out of order" patterns). Thus, instead of viewing them as a drawback we exploit their effect in order to increase the estimation accuracy and eliminate the limitations posed by the polar coordinates approach. Consequently, static reflections are allowed in this approach and the IRTX devices may transmit their patterns concurrently.

During real time operation, the current success rates retrieved by the target are compared with the grid node rates that were retrieved during the calibration stage. The comparison is based on the relative differences estimated by the equations (2) and (3):

$$d_{ij} = \begin{cases} \dfrac{v_j - r_{ij}}{v_j}, & if(v_j > r_{ij}) \\ \dfrac{r_{ij} - v_j}{r_{ij}}, & if(v_j \le r_{ij}) and(r_{ij} \ne 0) \\ 1, & if(v_j = 0) or(r_{ij} = 0) \end{cases} \tag{2}$$

$$D_i = \sum_j d_{ij} \tag{3}$$

The parameter v_j is the j-th position of the composite vector $C=[A\ A'\ B\ B']$ while r_{ij} is the corresponding value of the success rate vectors retrieved during calibration for node *i*. The individual success rate differences for all the *C* vector positions are summed up and the grid node *i* with the smaller D_i value is selected as the closer to the target position.

Although no model has been used to describe how the success rate of a pattern varies in neighbouring positions, it may be assumed that if the grid nodes are close enough it changes linearly between two successive nodes. Thus, if the success rate of a pattern at the nodes *i* and *j*, are r_i and r_j, the success rate *r* at the middle of these nodes is

$$r = (r_i + r_j)/2 \tag{4}$$

The selection of the grid node distance is critical and a trade off has to be made between the calibration speed and the estimation accuracy. If the node distance is very short, the high number of grid nodes will increase the duration of the calibration stage and the memory requirements. Moreover, if there are too many grid nodes then there will be an increased possibility that nodes with almost identical success rate identities will exist. These nodes may be confused in real time operation leading to erroneous position estimations. On the other hand, if a long distance is selected, then the assumption that the success rate of a pattern changes linearly between two neighbouring nodes is not valid.

In Fig. 9, the success rate of an expected (a) and an unexpected (b) pattern is drawn in an area of 1mX1m. A study of several 2D graphs like the ones presented in Fig. 9 leads to the conclusion that a grid with a 20cm node distance is appropriate for our system since the concept of the linear success rate variation between neighbouring nodes is preserved in most of the cases without significantly increasing the number of the grid nodes.
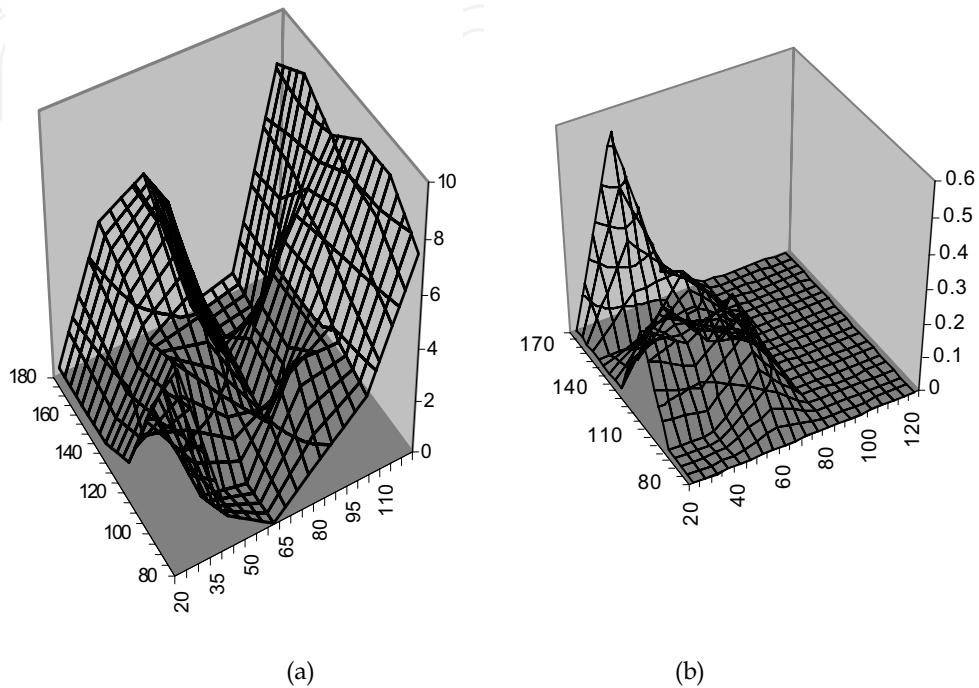
(a)   (b)

Fig. 9. Success rate variation in 2D of an expected (*a*) and unexpected (*b*) MOD7 pattern.

A refinement step follows the selection of the initial grid node in order to estimate more accurately the real position of the target. This step is basically an extension of the interpolation search algorithm in two dimensions. A new grid with the half node distance is defined by estimating the success rate identities of the new nodes using the equation (4). Consider for example Fig. 10 where the node *E0* of the initial grid is selected by the first comparison between the current and the calibration success rates. The success rates of the virtual nodes at the middle of *E0* and its neighbouring nodes *Ex* are estimated using equation (4) and their differences from the current rates are extracted using equations (2) and (3). The virtual node with the smallest D_i value is selected as the centre of the new grid (node E0′ in Fig. 10). The aforementioned procedure is repeated for the nodes of the new grid and a new position between *E0′* and the rest of the *Ex′* nodes is selected (*E0″*). If the definition of a new grid does not lead to a lower D_i value, then the recursive refinement procedure terminates.
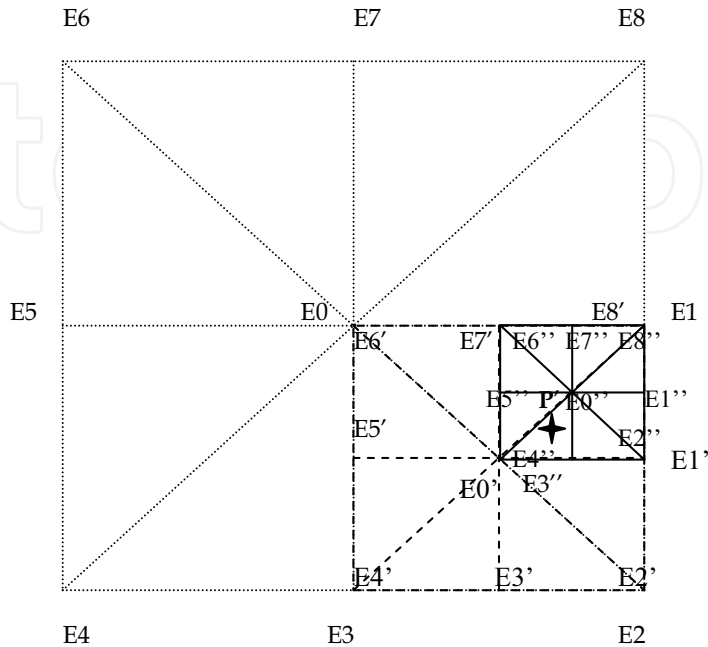
Fig. 10. The refinement step in the position estimation

4. Carrier Signal Options

As already mentioned in section 2, the patterns are transmitted over a carrier (F_c) in order to make it feasible for the receiver to abort the interfering infrared noise. A high pulse of an infrared pattern MODi should last for multiple carrier periods in order to reassure the effectiveness of the receiver bandpass filter:

$$H_i = k / F_c \qquad (5)$$

If $H=L$ the time needed to transmit the set of the identical MODi patterns is

$$T_i = M(P + 2ik / F_c) \qquad (6)$$

If T_{pream} is the duration of the preamble, the total time T that is needed to transmit all of the supported patterns is

$$T = T_{pream} + \sum_i M(P + 2ik / F_c) \qquad (7)$$

It is obvious from equation (7) that the position estimation procedure is slow if a low frequency carrier is chosen. For example, using the standard 38KHz carrier, the location of a position requires more than one second but low cost sensors with embedded carrier rejection circuitry can be employed at the side of the receiver. A significant reduction in this time can be achieved if a higher carrier frequency is used. In this case, higher processor speed, fast infrared emitters/sensors and a custom carrier filter are required.
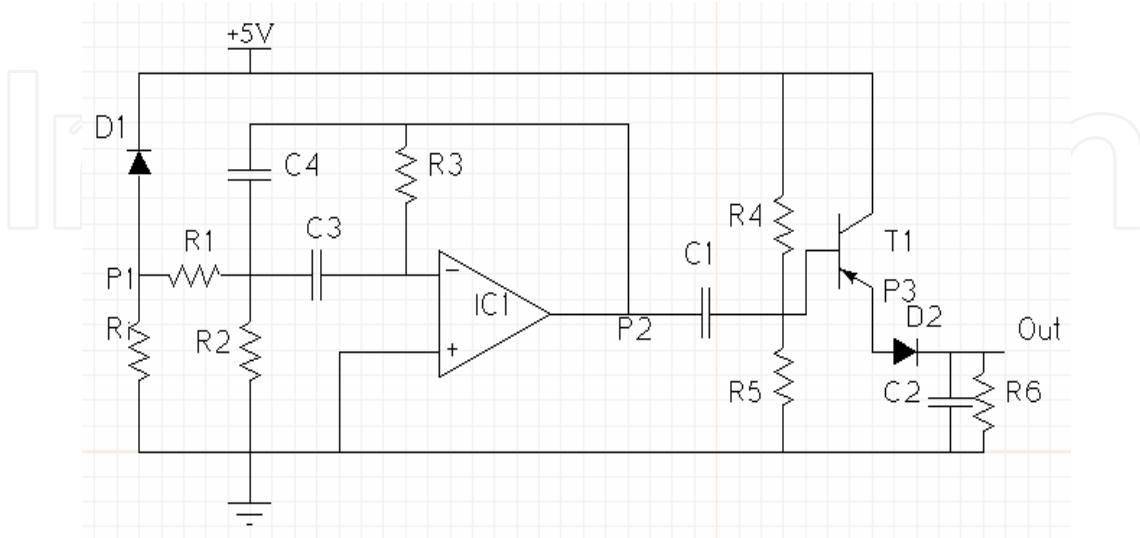
Fig. 11. A custom filter for high frequency carrier.

For example, the filter of Fig. 11 is used in this case. The infrared diode *D1* is connected inversely allowing a low current in the absence of infrared light (e.g., less than 50uA if the device model SFH203 is used). This current is increased to 80uA if infrared light falls on *D1*. The resistance *Ri* converts the current levels of *D1* to voltage input at the Multiple Feed Back Filter (MFBF) that consists of *R1, R2, C3, C4, R3* and *IC1*. If *B* is the desired bandwidth i.e., the frequency range where the signal is attenuated less than -3dB compared to the centre frequency f_c, the quality factor *Q* is defined as

$$Q = f_c / B \qquad (8)$$

If *G* is the desired filter gain (*Q* and *G* should not be much greater than 1) and the capacitors *C1* and *C2* are equal to a selected value *Cp*, the resistors *R1, R2* and *R3* can be estimated using the following equations (Lancaster, 1995):

$$R1 = Q / 2\pi f_c CpG \qquad (9)$$

$$R2 = Q /(2Q^2 - G)\pi f_c Cp \qquad (10)$$

$$R3 = Q / \pi f_c Cp \qquad (11)$$

The operational amplifier *IC1* is a high speed device capable of providing unity gain at much higher frequencies than f_c. For example, if the carrier frequency is 1MHz, the gain flatness of *IC1* should be kept less than 0.1dB for frequencies up to 60MHz. This requirement is harder to achieve if single power supply is used. The output of the *IC1* is amplified by *T1* through *C1* that isolates the MFBF filter from the amplification stage. The values of *C1* and *R5* are chosen in order to further attenuate the frequencies that are lower than f_c. The simple circuitry consisting of the components *D2, C2* and *R6* acts as an AM demodulator rejecting the current as can be seen in Fig. 12.

A Sensors System for Indoor Localisation
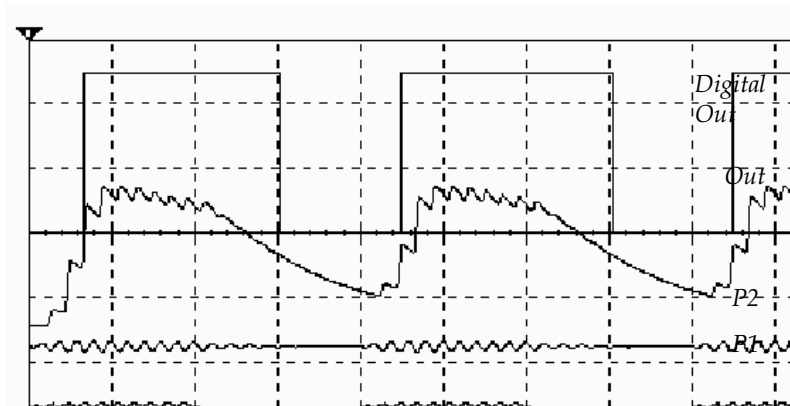of a Moving Target Based on Infrared Pattern Recognition

295

Fig. 12. The form of the received 1MHz signal at various stages of the MFBF filter.

Fig. 12 presents the behaviour in time of a 1MHz filter that attenuates by -30dB the signals with frequencies lower than 800KHz and greater than 1.2MHz. An input signal modulated at 1MHz appears at the junction *P1,* while *P2* is the output of the MFBF filter. Although the output of the demodulator (*Out*) is slightly rippling the signal can be safely sampled by a digital input.

Although several alternative passive or active filters could have been employed, the study of these options is out of the scope of this chapter. Using a 1MHz filter like the one presented above, the duration of the position estimation procedure can be reduced to less than 100ms.

5. Real Time Position Validation Rules

The results of successive position estimations may differ significantly even if the target stands still. This is due to the fact that dynamic noise and reflections have not been considered during the calibration stage. The rules described in this section can help the system reject the estimation results that differ significantly from the original target position (Petrellis et al, 2006c). Some of these rules can be used as estimation correction techniques or they may simply force the system to repeat the estimation process. As the target moves within the covered area, it performs position localisation processes at regular intervals T_s. Each process includes S successive position estimations. Thus, the duration of a localisation process is $S \cdot T$ where the time T was estimated by equation (7).

5.1 Limited Speed Rule (LSR)
The speed of the vehicle or the person that is considered as a target is always limited and slow. Thus, the distance R_s that may be walked between the successive localisation processes is also limited by the following relations:

$$V_{mn}(T_s + s \cdot T) \leq R_s \leq V_{mx}(T_s + s \cdot T) \tag{12}$$

The parameters V_{mn} and V_{mx} are the minimum and the maximum speed of the target respectively, while s is the sequence of the specific estimation within a localisation process

($1 \leq s \leq S$). There is always an upper limit for the speed of the target but not a lower one since the target may not move for a while. In this case, $V_{mn} = 0$ and the value of s defines disks that have as a common centre the position that has been selected by the previous localisation process. The coordinates estimated by the current position localisation process have to reside within these disks, otherwise they are rejected (Fig. 13a). If the target always moves ($V_{mn} > 0$), then homocentric rings that possibly overlap are defined by the relation (12) and the result of a position estimation has to reside within the corresponding ring as shown in Fig. 13b.

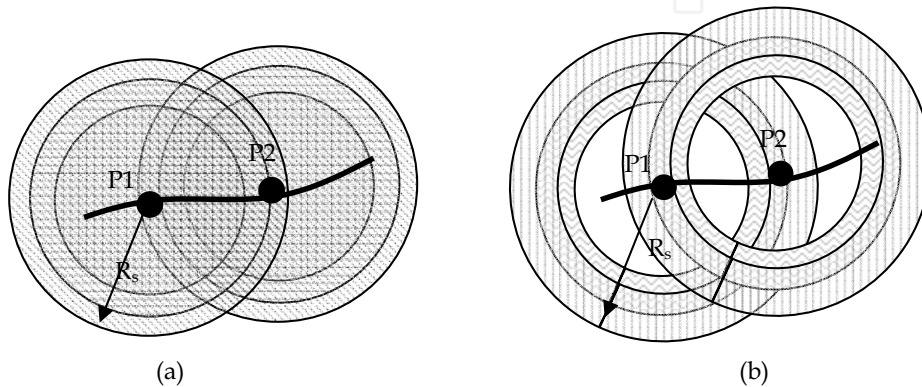(a)   (b)

Fig. 13. The limitations in the speed of the target define disks (a) or rings (b) where the acceptable positions reside.

The LSR rule can be used as a correction method if all the estimated positions are outside the limits of the disks or the rings. If P is the centre of the disk and P' is the closer estimated position outside the disk, then the point P'' selected. This is the point where the border of the disk intersects with the line that connects P with P' as shown in Fig. 14.
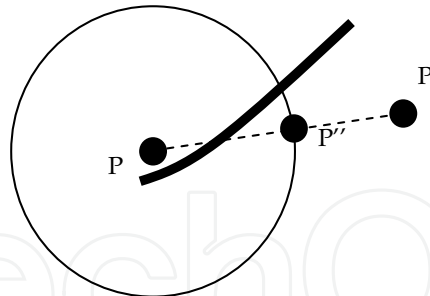

Fig. 14. Correction of the estimated results using LSR.

5.2 Neighbouring Regions Rule (NRR)

The way that the success rate of the patterns varies within the covered area may be used to divide this area in neighbouring regions. The concept of the NRR rule is that the target may cross neighbouring regions but cannot be found suddenly in a distant region. The NRR is actually a relaxed LSR rule and its basic purpose is the extension of the covered area by using more than 2 IRTX devices.

If the success rates presented in Fig. 9a and 9b are used, the regions *A, B, C* and *D* of Fig. 15 can be defined. The success rate class of *A7* in the range [0,10] is considered high (*H*) if it is more than 7, medium (*M*) if it is between 4 and 7, low (*L*) if it is between 1 and 4 and zero (*Z*) if it is less than 1. In a similar way, the success rate class of *B7* is defined as *H, M, L, Z* in the range [0,0.6]. Thus, the symbol *C(M,Z)* for example defines the region *C* where the success rates class of *A7* is *M* and *B7* is *Z*. A more accurate definition of the regions can be achieved if more than two success rate types are considered.
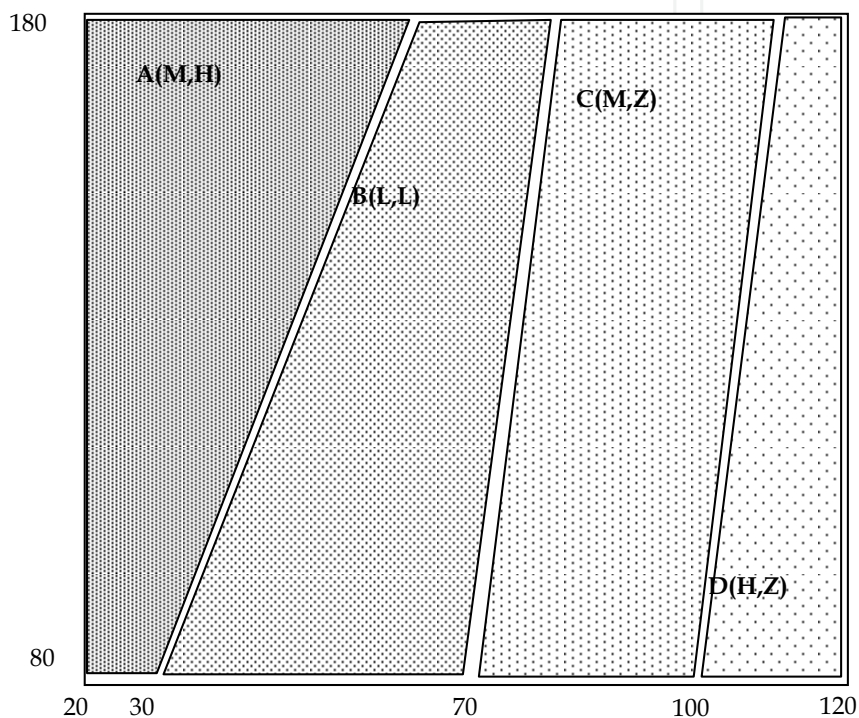

Fig. 15. Regions defined by the success rates of Fig. 9

If the speed of the target is low enough, it is assumed that it can only be found in the same or neighbouring regions in successive localisation processes. For example, if it is initially found in region *B*, the next acceptable position is allowed to be in regions *A, B* or *C* but not in *D*.

The area that is covered may be extended if the concept of the NRR rule is used with three or more IRTX devices. If the IRTX devices that are presented in Fig. 16 are used, the draft regions drawn in the same figure are defined. Each one of the IRTX1, IRTX2 and IRTX3 transmitters supports a different set of patterns. In this way, the target distinguishes the source of the patterns it receives. For example, if the reflections and the scrambling are negligible in the area of Fig. 16, the target receives high success rates from IRTX1 on $IRRX_A$ and lower success rates from IRTX2 on $IRRX_B$ when it is in region A. Similarly, in region B it receives high success rates from IRTX2 on $IRRX_B$ and lower from IRTX1 and IRTX3 on $IRRX_A$.
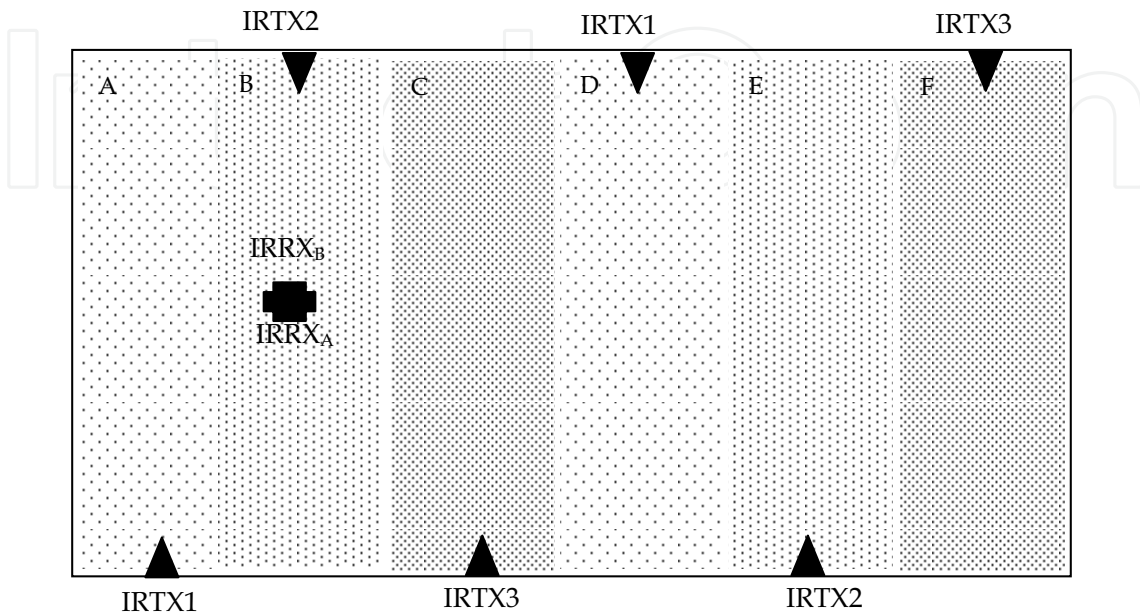
Fig. 16. Extending the area covered by using three or more IRTX devices.

In a real environment the regions neither have the regular shape presented in Fig. 16, nor the same size. They are defined using the information of 3D graphs like the ones presented in Fig. 9 and some distant regions have the same features if three types of IRTX devices are used repeatedly. The target should keep track of the regions that it has crossed in order to distinguish the exact region of its current position. For example, in regions *B* and *E* the target receives patterns with high success rate from IRTX2 on one IRRX device and lower success rates from IRTX1 and IRTX3 on the other IRRX device. This may cause a confusion of whether being in region *B* or *E*. Nevertheless, if it knows that the previous regions crossed were *C* and *D* in this specific turn, then the region *E* will be selected.

5.3 Direction Preserving Rule (DPR)

The third rule is based on the fact that the target is moving on the same rough direction most of the time. Although this is not true if for example the target follows a circular track, this rule can be very helpful in the general case. If *k* successive positions of the target are considered then *k-1* lines starting from the first position are defined as shown in Fig. 17. Two of these lines determine the wider angle that is considered as the rough direction where the next position is assumed to reside. The lower value that *k* can get is 3. In this case the two lines determine a single angle. For example, the positions *P0, P1* and *P2* determine the initial rough direction in Fig. 17. The next position (*P3*) should reside within the angle defined by *P0, P1* and *P2*. Then, the direction is updated using *P1, P2* and *P3* and the next position (*P4*) should reside within the angle defined by these three points.

The angle of *P0, P1* and *P2* is defined by:

$$\cos(P_1 \hat{P}_0 P_2) = \frac{(w_1 - w_0)(w_2 - w_0) + (l_1 - l_0)(l_2 - l_0)}{\sqrt{(w_1 - w_0)^2 + (l_1 - l_0)^2} \sqrt{(w_2 - w_0)^2 + (l_2 - l_0)^2}} \quad (13)$$

In the general case k points define $(k-1)(k-2)/2$ angles. The wider angle is chosen as the one with the lowest cosine value. The next position should reside within the wider angle. If $P0$, $P1$ and $P2$ define the wider angle then the next position Pn should comply with the following relations:

$$\cos(P1 \hat{P}0 Pn) \geq \cos(P1 \hat{P}0 P2) \quad (14)$$

$$\cos(Pn \hat{P}0 P2) \geq \cos(P1 \hat{P}0 P2) \quad (15)$$

The applicable values used for k are 4 to 6. Using $k=3$ is too restrictive since the angle defined is narrow and may often be 0°. On the other hand, using a high value for k leads to extremely wide angles that do not reject any of the estimated positions in a localisation process .
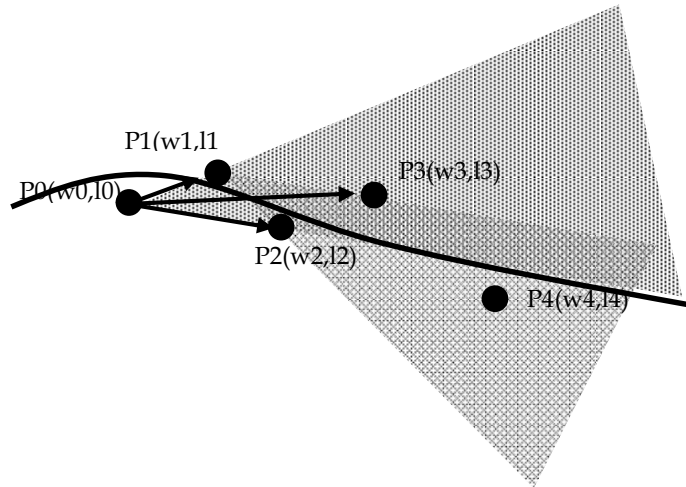

Fig. 17. Direction Preserving Rule

5.4 Steering Control Rule (SCR)

The SCR rule can be applied if the target is allowed to change his direction in specific angles. If Φ is the set of the allowed angles φ, then three successive positions $P1(w_1,l_1)$, $P2(w_2,l_2)$ and $P3(w_3,l_3)$ should satisfy the following relation:

$$\cos(\varphi) = \frac{(w_1 - w_2)(w_3 - w_2) + (l_1 - l_2)(l_3 - l_2)}{\sqrt{(w_1 - w_2)^2 + (l_1 - l_2)^2} \sqrt{(w_3 - w_2)^2 + (l_3 - l_2)^2}} \quad (16)$$

The SCR rule can also be used as an error correction rule if the closer position to an acceptable direction is rotated as shown in Fig. 18. In the general case presented in this

figure, four angles are allowed ($0°$, φ_1, φ_2 and φ_3). If $P3$ is the estimated position that is closer to an allowed direction (φ_2), the position $P3$ is rotated by equations (17)-(19) and the resulting position $P3'$ has the same distance d from $P2$ but in an acceptable direction.
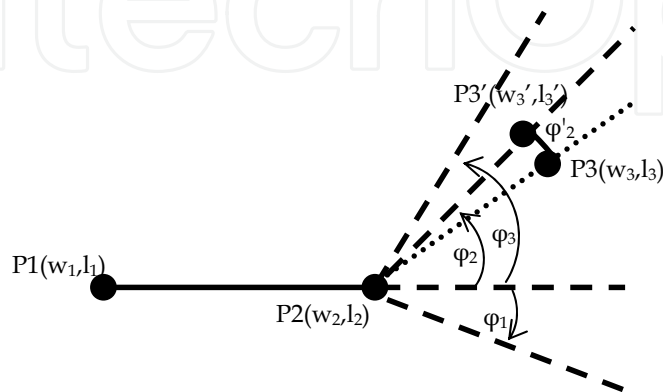

Fig. 18. Error correction using the SCR rule

$$w_3' = w_2 + d \cdot \cos \varphi_2 \tag{17}$$

$$l_3' = l_2 + d \cdot \sin \varphi_2 \tag{18}$$

$$d = \sqrt{(w_3' - w_2)^2 + (l_3' - l_2)^2} = \sqrt{(w_3 - w_2)^2 + (l_3 - l_2)^2} \tag{19}$$

6. Case Study

The experimental topology presented in Fig. 19 is used as a case study. Two IRTX devices are positioned in 1.8m horizontal and 3m vertical distance. Each IRTX device has two infrared emitting diodes of different type connected in parallel, placed in $45°$ angle. The external continuous line defines the range of at least one IRTX device signal. The area covered exceeds 15m^2 but the quality of the estimation results is not the same everywhere.

If a grid covering the whole area with long node distance (40cm) is considered then an estimation with an absolute error that is less than the half of the node distance (20cm) is acceptable. Each position localisation process carries out 5 successive estimations ($S=5$) and is considered successful if at least one of them has an absolute error of less 20cm. In this case, a 65% of the positions visited experimentally were localised successfully. If the four rules described in Section 5 are applied, then more than 90% of the positions visited are estimated successfully.

The absolute error can be reduced if a shorter node distance is used. In this case, it is difficult to cover the whole area since the number of grid nodes is significantly increased leading to a longer calibration time and possibly to poor results as already described in

Section 3. If we focus on the 1m² area in the dotted square of Fig. 19 and use a 20cmX20cm grid, then all the positions visited are localised with an error of less than 10cm.
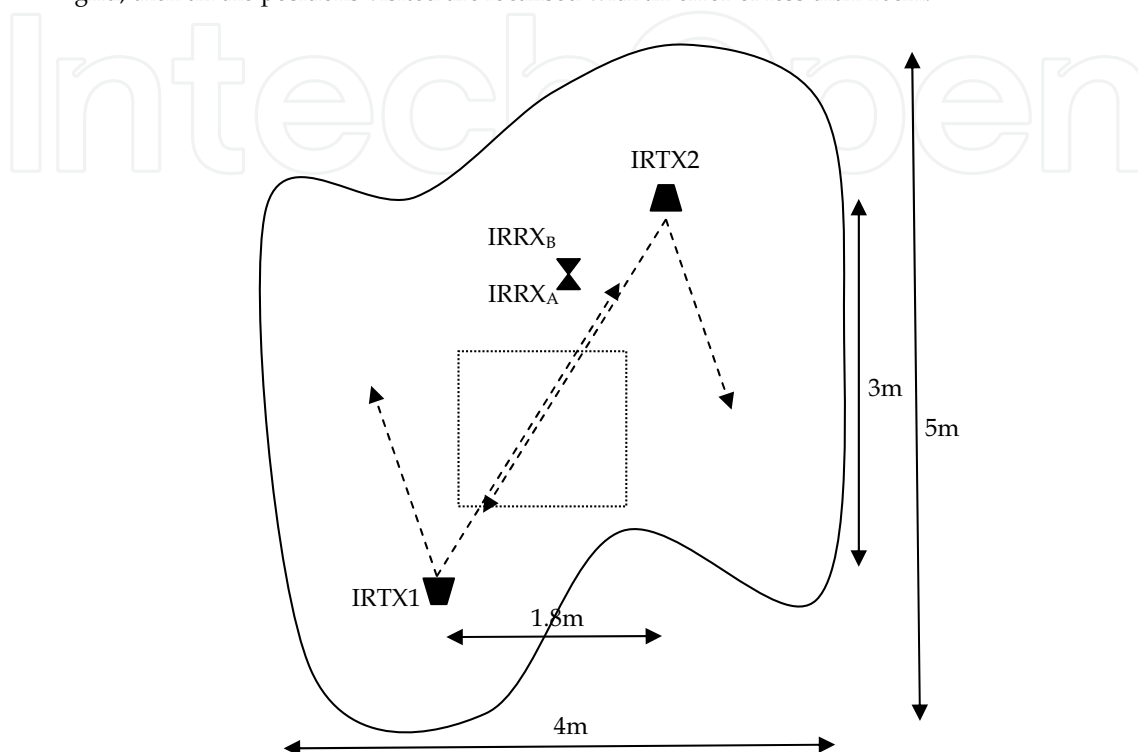

Fig. 19. The area covered by two IRTX devices

The dotted area of Fig. 19 and the corresponding success rate variation of Fig. 9 and Fig. 15 are used in order to describe how the LSR, NRR and DPR rules of Section 5 are used. The SCR is not applied since the target is free to turn in any direction. The real track of the target is the one depicted with the bold continuous line in Fig. 20. The dashed circles indicate the maximum LSR distance that the target was allowed to walk between two localisation processes. For simplicity reasons we only refer here to multiple estimation results of a localisation process when they are used by the position restriction rules.

The LSR and NRR rules are applied first while the DPR rule is used in a supplementary way. If we assume that the positions *P1, P2* and *P3* have already been estimated, the position *P4* is selected as a next step instead *P4'* since the last one deviates the LSR rule. Note that both of *P4* and *P4'* are compliant with the NRR rule but this is not a problem since the NRR is a relaxed LSR rule targeted for the potential extension of the covered area. In the next localisation process none of the estimated positions complies to any of the three rules. If *P5'* is one of the unaccepted positions that is closer to *P4* then the position *P5* is the result of the error correction performed by LSR. In the following localisation process both *P6* and *P6'* are acceptable by LSR and NRR. In this case, the DPR rule can be used to abort *P6'*. The previous positions *P2, P3, P4* and *P5* (i.e., *k=4*) are used by the DPR rule in order to define the rough direction depicted by the dotted lines starting from *P2* in Fig. 20. Finally, the two

alternative positions: *P7′* and *P7′′* deviate both the LSR and the DPR rules in the next localisation process but *P7′* is compliant with NRR. Thus, *P7′* is selected in the LSR error correction method that leads to *P7* as the last position of the target in this example. The bold-dashed line of Fig. 20 is the estimated target track.
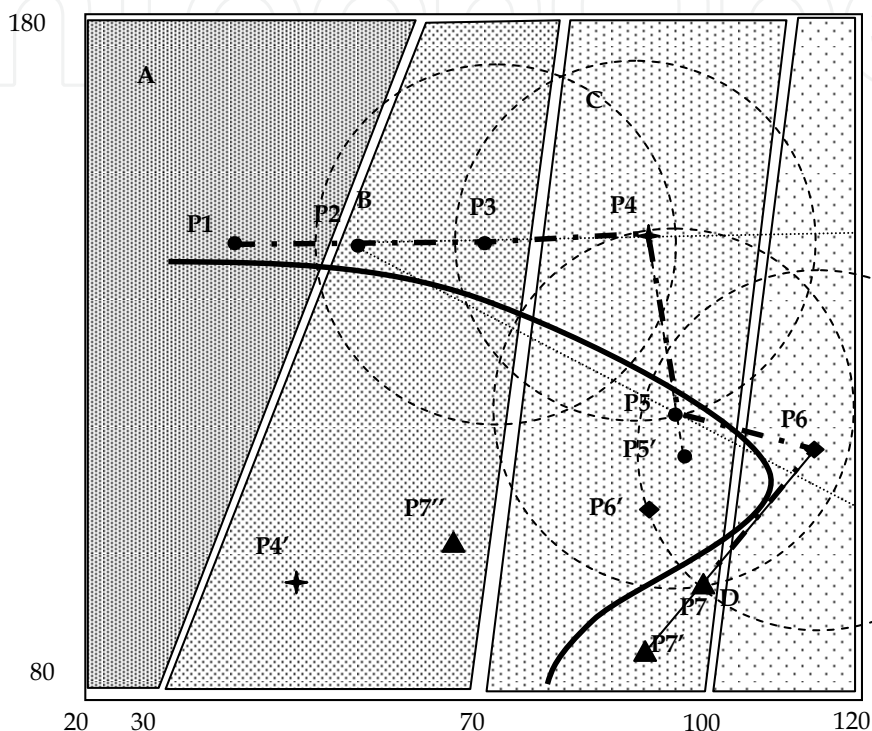

Fig. 20. The use of the LSR, NRR and DPR rules.

7. Conclusions

A novel method for the indoor localisation of a target was presented in this chapter. This method is based on measuring the number of the digital infrared patterns received by the target in a specific time interval (success rate). At least two transmitting devices are placed around the covered area that exceeds 15m², while a pair of infrared receivers are mounted on the target. This area is supposed to be covered by a virtual grid and can be further extended if more transmitters are employed. The grid nodes are visited by the target during a calibration stage when it familiarises with the retrieved success rates. At real time operation the closer grid node is selected and a refinement step based on a 2D interpolation search follows leading to a more accurate position estimation.

The absolute error that can be achieved is less than 10cm but may vary significantly if successive estimations are carried out at the same position. Four deterministic rules are described in order to abort the false estimations caused by dynamic noise and stabilise the

estimation procedure. The speed of the localisation procedure depends on the frequency of the carrier that is used in order to shield the patterns from the interference of other infrared sources. The rather long estimation time that is needed for a standard 38KHz carrier frequency can be reduced to less than 100ms if a higher frequency is selected. The design of a custom 1MHz carrier filter was presented as an example.

Future work will focus on experimenting with various infrared pattern structures and system topologies in order to increase the estimation speed and accuracy and expand the area covered. Finally we will attempt to utilise the concept of our system in the case of targets with more degrees of freedom (moving in three dimensions, rotating etc).

8. References

Arana, S. Arana, N., Gracia, J. & Castano, E., High Sensitivity Linear Position Sensor Developed Using Granular Ag-Co, Giant Magnetoresistances. *Sensors And Actuators,* A 123-124, 2005, pp. 116-121.

Arras, K., Tomatis, N., Jensen, B. & Siegward, R., Multisensor On-the-Fly Localisation : Precision and Reliability for Applications. *Elsevier Robotics and Autonomous Systems*, 43(2001), pp. 131-143.

Aytac, T. & Barshan, B., Simultaneous Extraction of Geometry and Surface Properties of Targets Using Simple Infrared Sensors. *Optical Engineering,* 43(10), Oct. 2004, pp. 2437-2447

Bates, D. & Watts, D. (1988). *Nonlinear Regression Analysis and Its Applications,* Wiley Series in Probability and Statistics, Hoboken, NJ

Benet, G, Blanes, F., Simo, J. & Perez, P. Using Infrared Sensors for Distance Measurement in Mobile Robots. *Robot Autonomy Systems,* Vol. 30, 2002, pp. 255-266

Bicho, E., Mallet, P. & Schoner, G. Target Representation on an Autonomous Vehicle with Low Level Sensors, *Int. Journal of Robotics Research,* Vol. 19, No. 5, May 2000, pp. 424-447

Borenstein, J. Everett, B. & Feng, L. (1996). *Navigating Mobile Robots: Systems and Techniques*, A.K. Peters Ltd Wellesley, MA

Clerentin A., Delahoche, A., Brassart, E. & Drocourt, C. Self Localisation: A New Uncertainty Propagation Architecture. *Elsevier Robotics and Autonomous Systems*, 51(2001), pp. 151-166

Flora, C., Ficco, M., Russo, S. & Vecchio, V. Indoor and Outdoor Location Based Services for Portable Wireless Devices. *Proceedings of 1st IEEE Int. Workshop on Services and Infrastructure for Ubiquitous and Mobile Internet,* pp. 244-250, June 2005, Columbus OH

Gramegna, T., Venturino, L., Cicirelli, G., Attolico, G. & Distante, A. Optimisation of the POSIT Algorithm for Indoor Autonomous Navigation. *Elsevier Robotics and Autonomous Systems*, 48(2004), pp. 145-162

Holmberg, P. Ultrasonic Sensor Array for Positioning and Rotation Estimates of Planar Surfaces. *Sensors and Actuators A*, 44(1994), pp. 37-43

Jin, T., Lee, J. & Tso, S. A New Space and Time Sensor Fusion Method for Mobile Robot Navigation. *Wiley Journal of Robotics Systems*, 21(7), 2004, pp. 389-400

Kosel, J. Pfutzner, H., Mehnen, L., Kaniusas, E., Meydan, T., Vazquez, N., Rohn, M., Merlo, A. & Marquardt, B. Non Contact Detection of Magnetoelastic Position Sensors. *Elsevier Sensors and Actuators A*, 123-124 (2005), pp. 349-353

Kzecka, J. Li, F. & Yang, X. Global Localisation and Relative Positioning Based on Scale Invariant Keypoints. *Elsevier Robotics and Autonomous Systems,* 52(2005), pp. 27-38

Ladd, A., Bekiris, K., Rudys, A., Kavraki, L. & Wallach, D. Robotics Based Location Sensing Using Wireless Ethernet. *Wireless Networks,* Vol. 11, No. 1-2, Jan 2005, pp. 189-204

Lancaster, D. (1995). *Active Filter Cookbook.* 2nd Edition Newnes-Elsevier Science, MA

Minami, M., Fukuju, Y., Hirasawa, K., Yokoyama, S., Mizumachi, M., Morikawa, H. & Aoyama, T. Dolphin: A Practical Approach for Implementing a Fully Distributed Indoor Ultrasonic Positioning System. *Lect Not Comp Sci,* 3205, 2004, pp. 347-365

Miura, J., Negishi, Y. & Shirai, Y. Adaptive Robot Speed Control by Considering Map and Motion Uncertainty. *Elsevier Robotics and Autonomous Systems,* 54(2006), pp. 110-117

Novotny, P. & Ferrier, N. Using Infrared Sensors and the Phong Illumination Model to Measure Distances. *Proceedings of the IEEE Int. Conf. On Robotics and Automation,* pp. 1644-1649, 1999, Detroit MI

Petrellis, N. Konofaos, N. & Alexiou, G. Testing IR photon sensors for target localisation applications. *Proceedings of the 1st Int. Workshop on Advances in Sensors and Interfaces.* Aula Magna "Attilo Alto", pp. 153-158, Apr 2005, Bari, Italy

Petrellis, N. Konofaos, N. & Alexiou, G. Target Localisation Utilising the Success Rate in Infrared Pattern Recognition. *IEEE Sensors Journal*, 6(5), 2006, pp. 1355-1364

Petrellis, N. Konofaos, N. & Alexiou, G. Position Estimation on a Grid Based on Infrared Pattern Reception Features. *Int. Workshop on Ubiquitous Computing (IWUC),* pp. 21-28, May 2006, Paphos, Cyprus

Petrellis, N. Konofaos, N. & Alexiou, G. Utilising Infrared Pattern Recognition Features for Indoor Localisation Validated by Future Position Restrictions. 2nd IET Int. Conf. On Intelligent Environments (IE '06), pp. 307-311, July 2006, Athens, Greece

Porta, J. & Krose B. Appearance-based Concurrent Map Building and Localisation. *Elsevier Robotics and Autonomous Systems,* 54(2006), pp. 159-164

Prigge, E. & How, J. Signal Architecture for Distributed Magnetic Local Positioning System. *IEEE Sensors Journal.* Vol. 4, No. 6, 2004, pp. 864-873

Schlageter, V., Besse, P., Popovic, R. & Kucera, P. Tracking System with 5deg of Freedom Using a 2D Array of Hall Sensors and a Permanent Magnet. *Elsevier Sensors and Actuators A,* 92, 2001, pp. 37-42

Se, S., Lowe, D. & Little, J. Mobile Robot Localisation and Mapping With Uncertainty Using Scale Invariant Visual Landmarks. *Int. Journal of Robotics Research.* Vol. 21, No. 8, 2002, pp. 735-758

Thrun, S. A Probabilistic On Line Mapping Algorithm for Team of Robots. *Int Journal of Robotics Research.* Vol. 20, No. 5, May 2001, pp. 335-363

Tovar, B., Gomez, L., Cid, R., Miranda, M., Monroy, R. & Hutchinson, S. Planning Exploration Strategies for Simultaneous Localisation and Mapping. *Elsevier Robotics and Autonomous Systems.* 54(2006), pp. 314-331

Ullate, L., Sanchez, M., Villanueva, E., Parilla, M. & Anaya, J. A Three-Transducer Ultrasonic System for Object Location in the Air. *Elsevier Sensors and Actuators A*, 37-38(1993), pp. 391-396

Victorino A., Rives, P. & Borelly, J. Safe Navigation for Indoor Mobile Robots Part II: Exploration, Self Localisation and Map Building. *Int. Journal of Robotics Research.* Vol. 22, No. 12, Dec 2003, pp. 1019-1039

Scene Reconstruction Pose Estimation and Tracking

Edited by Rustam Stolkin

This book reports recent advances in the use of pattern recognition techniques for computer and robot vision. The sciences of pattern recognition and computational vision have been inextricably intertwined since their early days, some four decades ago with the emergence of fast digital computing. All computer vision techniques could be regarded as a form of pattern recognition, in the broadest sense of the term. Conversely, if one looks through the contents of a typical international pattern recognition conference proceedings, it appears that the large majority (perhaps 70-80%) of all pattern recognition papers are concerned with the analysis of images. In particular, these sciences overlap in areas of low level vision such as segmentation, edge detection and other kinds of feature extraction and region identification, which are the focus of this book.

How to reference

In order to correctly reference this scholarly work, feel free to copy and paste the following:

Nikos Petrellis, Nikos Konofaos and George Alexiou (2007). A Sensors System for Indoor Localisation of a Moving Target Based on Infrared Pattern Recognition, Scene Reconstruction Pose Estimation and Tracking, Rustam Stolkin (Ed.), ISBN: 978-3-902613-06-6, InTech, Available from:
http://www.intechopen.com/books/scene_reconstruction_pose_estimation_and_tracking/a_sensors_system_for_indoor_localisation_of_a_moving_target_based_on_infrared_pattern_recognition

INTECH
open science | open minds